Practical range and energy loss of 0.1–3-keV electrons in thin films of N_2, O_2, Ar, Kr, and Xe

Arnold Adams and P. K. Hansma
Department of Physics and Quantum Institute, University of California, Santa Barbara, California 93106
(Received 10 June 1980)

Thin solid films of N_2, O_2, Ar, Kr, and Xe were condensed on a cooled (11 K) sapphire substrate and then bombarded by monoenergetic electrons. The fluorescence intensity of the Cr^{3+} color center in sapphire ($\lambda = 693$ nm) was measured as a function of film thickness and electron energy to determine the electron practical range and effective energy loss (dE/dz). The Cr^{3+} intensity versus primary-electron-energy and film-thickness curves also yield information on the production of secondary electrons. The results are compared to an extrapolation of Bethe-Bloch theory to low energies for total range and energy loss (dE/ds) and to the electron-gas statistical model of Tung, Ashley, and Ritchie for low-energy electrons.

I. INTRODUCTION

There has been much work done in measuring and calculating the range, stopping power, and inelastic mean free path of low-energy ($E < 10$ keV) electrons in solids.[1–15] The recent articles by Ashley, Tung, and Ritchie[1,2] present an electron-gas statistical model for understanding electron inelastic mean free paths and energy losses in solids. Inelastic mean-free-path data are collected in the review articles of Powell,[3] Brundle,[4] and Lindau and Spicer.[5] A review of the many techniques used to measure inelastic mean free paths is contained in Powell's paper. Practical range measurements are contained in Refs. 8–15. Theoretical electron scattering amplitudes and spin polarizations for 27 elements[16,17] are also available. At this time, however, the experimental data have most often been obtained for metals, semiconductors, and thin metal oxide films, and have been plagued by large uncertainties.[3] Also, the measurements of practical range have been done at high energies[10–15] due to the difficulty in preparing films thin enough for low-energy electrons to penetrate. There has also been a difficulty in that theory yields R_s, the total path length of the primary electron while experiments give the practical range, R_z, which is the maximum film thickness that an electron of a given energy can penetrate. This problem was treated theoretically as early as 1938 by Bethe, Rose, and Smith[18] and more recently by Jacob and Bethe.[19] Surprisingly, there have been no quantitative comparisons between theory and experiment for R_z at low energies.

This paper presents electron practical range, R_z, effective stopping power, (dE/dz), and some qualitative information on the production of secondary electrons in the energy range 0.1–3 keV for insulators (N_2, O_2, Ar, Kr, and Xe) at low temperature. R_z is obtained by measuring the exponential decay constant of the intensity of the Cr^{3+} sapphire color center as a function of film thickness for a given electron energy. dE/dz is obtained by taking the inverse slope of the R_z vs E curves.

II. EXPERIMENTAL

The apparatus has been described in more detail elsewhere.[20] A schematic diagram is shown in Fig. 1. The experiments were carried out in a bakeable ion-

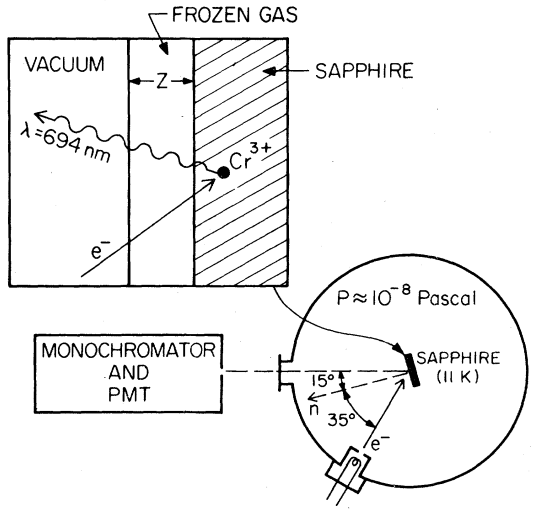

FIG. 1. Schematic diagram of the apparatus used to study electron range and energy loss in condensed solids. The inset shows the sapphire substrate and condensed gas of thickness z.

pumped and titanium sublimation-pumped ultrahigh-vacuum system with typical operating pressures below 7×10^{-8} Pa ($\sim 5 \times 10^{-10}$ Torr). This pressure corresponds to the order of 1 impurity monolayer or less striking the substrate per hour. This rate of impurity buildup was considered to have a negligible effect on the experiments, even if the sticking coefficient of the residual gases was unity.

An electron gun, residual gas analyzer, two variable leak gas inlets, and quartz observation windows were all directed at the chemically cleaned single-crystal sapphire substrate which was attached to a UHV modified two-stage helium recirculating refrigerator. Temperature was measured by a calibrated iron-doped gold versus Chromel thermocouple. The experiments were performed at 11.0 ± 1.0 K. A photoelectric detection system, quartz optics, 0.25-m monochrometer (0.4-mm slits), and chart recorder were used to measure the Cr^{3+} color-center intensity.

The thickness of the frozen gas film deposited on the substrate was determined by counting interference fringes from specularly reflected Hg pen lamp light ($\lambda = 253.65$ nm) directed at 15° from the substrate normal into the monochrometer and photomultiplier tube (PMT) for a given exposure (pressure × time) of the substrate to gas. For N_2, the measured points fell on a straight line with slope 1100 nm/Pa sec. This thickness versus exposure calibration factor was independent of deposition rate over the range 0.08 to 1.5 nm/sec (7×10^{-5} to 130×10^{-5} Pa). We used this measured calibration factor at the lower exposure rates to estimate the thickness of our thinner films of N_2. The ion gauge was calibrated for N_2 and no corrections were made for the other gases. Similar exposure calibration factors were obtained for the other gases: O_2, 820 nm/Pa sec; Ar, 620 nm/Pa sec; Kr, 380 nm/Pa sec; Xe, 310 nm/Pa sec. Previous work[21] showed the sticking coefficient of all gases used in this study to be approximately unity on a 10-K surface.

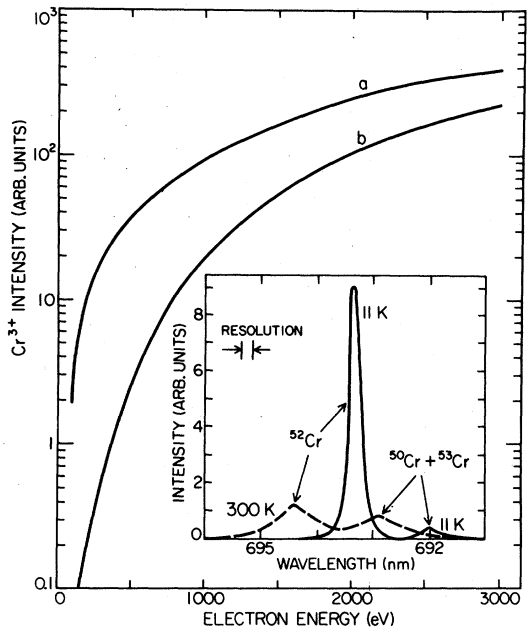

FIG. 2. Intensity of the $^{52}Cr^{3+}$ color center as a function of primary-electron energy. Curve a was taken with no silver deposited on the surface, while curve b was taken with a thin layer of silver deposited on the sapphire surface. The inset shows the frequency and temperature dependence of the color center.

The following was typical of most experiments. The UHV system was pumped below 7×10^{-8} Pa and the residual gases checked to be sure there were no leaks. The refrigerator was turned on and at 10 K a known thickness of research-grade gas deposited. Thicker layers were deposited in subsequent runs after first desorbing the previous frozen gas layer by heating to 100 K. The electron gun excited the Cr^{3+} sapphire color center with 0.1–3-keV electrons (0.5 μA) incident at 35° to the substrate normal. The energy flux over the approximately 0.2-cm^2 excited area was 0.25–7.5 mW/cm^2, depending on the incident electron energy. Some of the runs had a thin layer ($\sim$4 nm) of nearly transparent silver deposited on the sapphire. Its main effect was to reduce the number of secondary (low-energy) electrons measured. This was particularly helpful in measuring the intensity versus thickness decay constants of the rare gases. Figure 2 shows the intensity of the sapphire color center as a function of primary electron energy for no deposited frozen gas. The inset shows the frequency and temperature dependence of the color center. Curves a and b are measurements of the $^{52}Cr^{3+}$ color-center intensity at 11 K. Curve b is for a thin layer of silver deposited on the sapphire.

III. DISCUSSION OF RESULTS

Figures 3–7 give three-dimensional (3D) representations of the normalized color-center intensity versus frozen-gas thickness for various initial electron energies. The normalized intensity is the actual intensity $[I(z,E_0)]$ divided by the intensity at zero thickness $[I(0,E_0)]$ for a given incident electron energy E_0. Normalized intensity can be converted to relative intensity by multiplying by curve a in Fig. 1 for N_2 and O_2 or curve b for Ar, Kr, and Xe. The qualitative contributions to the intensity from secondary electrons are more easily seen using 3D plots of normalized intensity versus thickness versus incident electron energy than in 2D plots of intensity versus thickness or intensity versus electron energy. The secondary electrons cause the intensity to increase for larger values of thickness. The effects are largest at

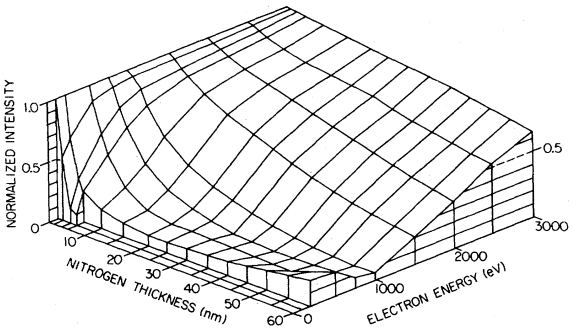

FIG. 3. Three-dimensional representation of the normalized color-center intensity vs solid-N_2 thickness vs incident electron energy. Normalized intensity can be converted to actual intensity (arb. units) by multiplying by curve a in Fig. 2.

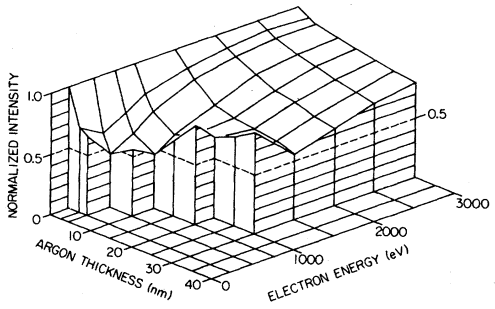

FIG. 5. Three-dimensional representation of the normalized color-center intensity vs solid-Ar-thickness vs incident electron energy. Note the rapid increase in intensity with an increase in thickness at large thicknesses. This effect is due to the production of secondary electrons. At low energies, the intensity at large values of the thickness reaches a maximum of a few times the intensity at zero thickness and then decreases slowly with further increases in thickness.

low energies and for the rare gases, in agreement with calculations of Opal *et al.*[22] All of the frozen gases exhibit initial exponential decays of intensity with thickness for a given incident electron energy which become more linear as the incident electron energy increases. We suppose that the change from exponential decay to linearity comes about due to the decreasing cross section for production of secondary electrons with increasing energy.[22] The practical range has been determined in the past by extrapolating to zero intensity the linearly decaying portion of the graph of either intensity versus thickness at constant energy or intensity versus energy at constant thickness. To obtain a similar value of the practical range at lower energies we take the inverse slope of the intensity versus thickness curve at zero thickness where no secondary-electron contribution is present. The inverse slope is the characteristic exponential decay length and also the practical (extrapolated) range of the electrons since the inverse slope is the intersection of the extrapolated line with the energy axis.

All results were reproducible to within about $\pm 15\%$ except for O_2 which were reproducible to within $\sim \pm 30\%$. The difficulty with O_2 was that there was a large-intensity time dependence. The data shown in Fig. 4 were taken after 1–5 sec of irradiation of the O_2 film. After 15 sec of irradiation the intensities for high energies stabilized but were drastically reduced (factor of 3) giving ranges much less than for short times of irradiation. This indicates either electronic structural change in the O_2 film or charging of the film due to a less than unity secondary-electron-emission coefficient. The N_2 and Ar but not Kr or Xe films had small-intensity time dependences that were entirely attributable to hole burning

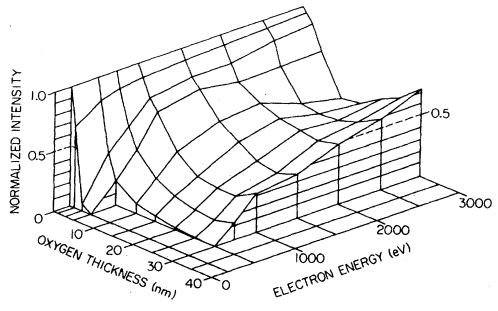

FIG. 4. Three-dimensional representation of the normalized color-center intensity vs solid-O_2 thickness vs incident electron energy. The O_2 curves showed a strong time dependence.

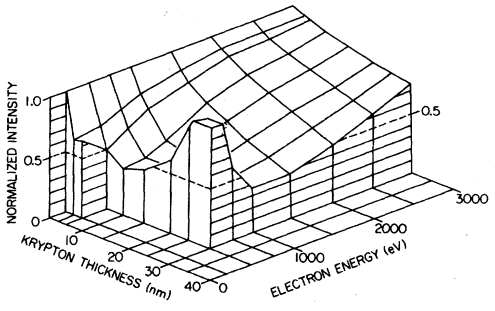

FIG. 6. Three-dimensional representation of the normalized color-center intensity vs solid-Kr thickness vs incident electron energy. These curves exhibit secondary-electron effects similar to Ar in Fig. 5.

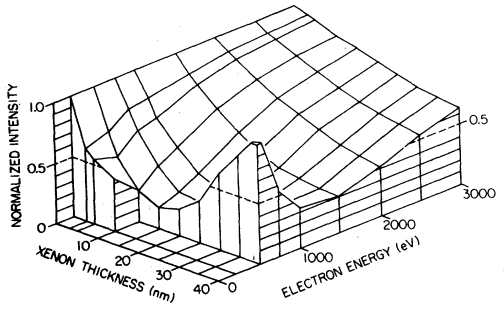

FIG. 7. Three-dimensional representation of the normalized color-center intensity vs solid-Xe thickness vs incident-electron energy. These curves exhibit secondary-electron effects similar to Ar and Kr.

in the films at a rate of ~2 nm/min. This effect was negligible since each measurement took about 2 seconds.

Figures 8–12 show the experimental values of the practical range, R_z, and effective stopping power dE/dz, along with an extrapolation to low energies of

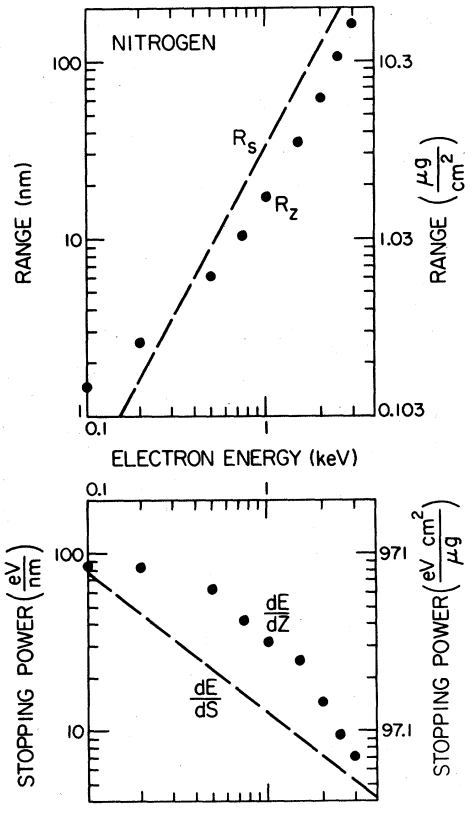

FIG. 8. Experimental values of the practical range, R_z, and effective stopping power, dE/dz, for N_2 as a function of incident-electron energy. R_s and dE/ds were obtained from an extrapolation of Bethe-Block theory to low energies.

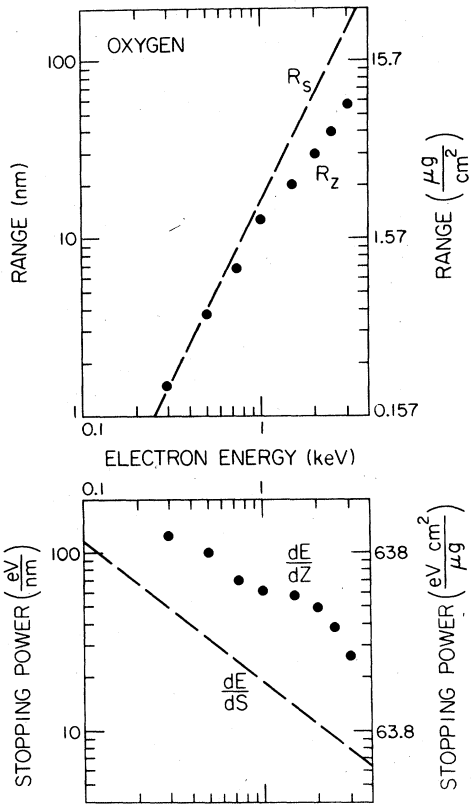

FIG. 9. Experimental values of R_z and dE/dz for O_2 as a function of incident-electron energy. Bethe-Bloch values of R_s and dE/ds are also given.

Bethe-Block theory for R_s and dE/ds obtained from Pages *et al.*[23] Practical-range units are given in both nm (the experimentally accessible quantity for large film thicknesses) and in g/cm^2 as determined by assuming that the films have bulk density. The units of g/cm^2 may actually be more accurate than nm for very thin films if the sticking coefficient is a constant as a function of thickness. In any case, the difference in bulk and film density is likely to be small. Effective-stopping-power units are also given in eV/nm and eV cm^2/g. Bulk densities were obtained from Refs. 24 and 25.

It has been pointed out[26,27] that Bethe-Bloch theory should still be valid to within ~10% at energies as low as 1 keV. Comparisons of the electron-gas statistical model of Ashley *et al.*[1,2] with extrapolations of Bethe-Bloch theory yield similar values of the stopping power (dE/ds) and inelastic mean free path for incident electrons with energies greater than 1 keV. For energies between ~0.2 and 1 keV, Bethe-Bloch theory gives a slight overestimate of the stopping power (hence underestimation of the range) relative to the electron-gas statistical model. For ener-

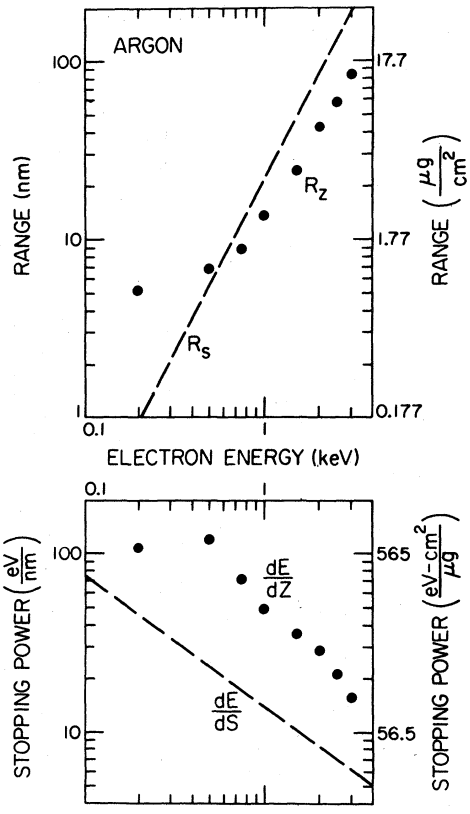

FIG. 10. Experimental values of R_z and dE/dz for Ar as a function of incident-electron energy. Bethe-Bloch values of R_s and dE/ds are also given.

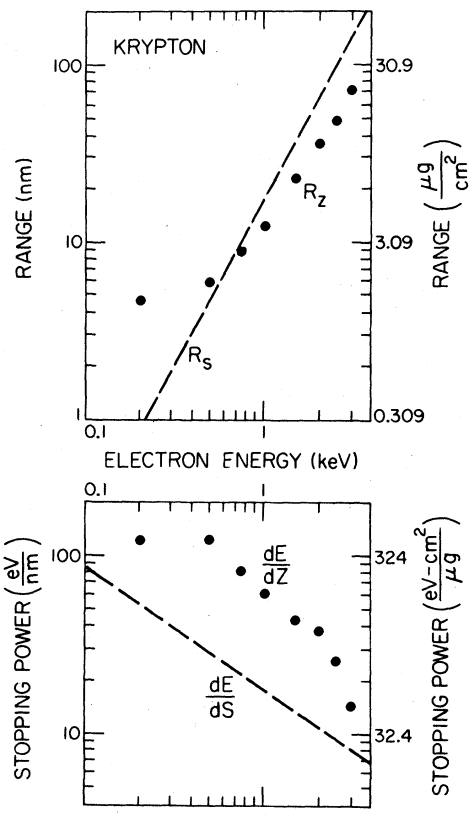

FIG. 11. Experimental values of R_z and dE/dz for Kr as a function of incident-electron energy. Bethe-Bloch values of R_s and dE/ds are also given.

gies less than about 0.1 keV this overestimation of the stopping power (underestimation of the range) becomes severe. The source of this discrepancy is that Bethe-Bloch theory is based on scattering by free electrons, and below 1 keV effects of electrons binding to nuclei become important. A bound electron is a less efficient scatterer of an incident electron if the incident electron energy is below the binding energy.

Theoretical comparisons of Bethe-Bloch theory with the electron-gas statistical model over the energy range of our experiments (0.1–3 keV) yield approximately the same results for dE/ds but not for R_s since

$$R_s = \int_0^{E_0} \left[\frac{dE}{ds}\right]^{-1} dE \ , \tag{1}$$

and dE/ds is underestimated by Bethe-Bloch theory in the energy range 0–0.1 keV. This effect is pronounced at low energies ($E_0 \lesssim 0.5$ keV) where the experimental value of R_z approaches or is above the R_s curve from Bethe-Bloch theory (see Figs. 8–12; R_s does not take account of multiple scattering and so should always be above the R_z curve).

To obtain theoretical values of the practical range to compare to experimental values for low-energy electrons requires a calculation of dE/ds and the transport mean free path, λ_t, from the electron-gas statistical model. These must then be applied to the problem of an electron being scattered through a film of thickness z, taking into account the total differential scattering cross section as a function of energy.

At low energies (less than 10 keV) the inelastic differential scattering cross section is an appreciable part of the total scattering cross section as can be seen from comparisons of the elastic transport mean free path, λ_t, and the inelastic mean free path. At 3 keV in N_2, λ_t is about 40 nm and the inelastic mean free path is about 5 nm.

Unfortunately, total differential cross sections for condensed gases have not been measured in the energy range 0–3 keV, to our knowledge.[16,17,28] Even if they were available, it would be tedious to do the numerical integrals necessary to make estimates with

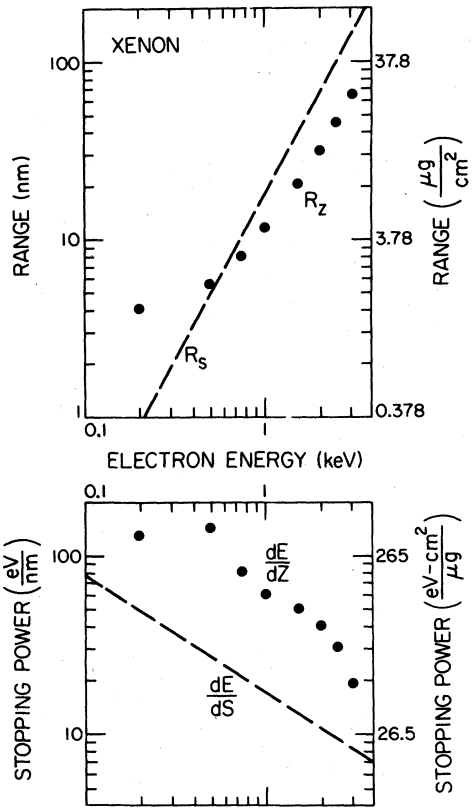

FIG. 12. Experimental values of R_z and dE/dz for Xe as a function of incident-electron energy. Bethe-Bloch values of R_s and dE/ds are also given.

existing theories. Theoretical work that bypassed this difficulty would be of great interest.

IV. SUMMARY

The intensity of the electron-excited Cr^{3+} color center has been measured as a function of frozen gas (N_2, O_2, Ar, Kr, and Xe at 11 K) thickness and electron energy from 0.1–3 keV. The practical range, R_z, of the incident electrons has been determined by measuring the exponential decay constant of the intensity versus film-thickness curves at constant energy and compared to theoretical R_s values. The R_z vs E_0 curves are differentiated to give an effective stopping power, dE/dz, and compared to theoretical values of dE/ds. The limitations of Bethe-Bloch theory at low energy are discussed and compared to the general results of the electron-gas statistical model of Tung, Ashley, and Ritchie. Difficulties in applying a theory of multiple scattering to our results were also discussed.

ACKNOWLEDGMENTS

We would like to thank Professor H. A. Bethe and Professor H. Metiu for useful conversations on the theoretical interpretations of our data. One of us (P.H.) would like to thank the A. P. Sloan Foundation for a fellowship. This work was supported by the NSF, Grant No. DMR76-83423.

[1]J. C. Ashley, C. J. Tung, and R. H. Ritchie, Surf. Sci. 81, 409 (1979).
[2]C. J. Tung, J. C. Ashley, and R. H. Ritchie, Surf. Sci. 81, 427 (1979).
[3]C. J. Powell, Surf. Sci. 44, 29 (1974).
[4]C. R. Brundle, J. Vac. Sci. Technol. 11, 212 (1974).
[5]I. Lindau and W. E. Spicer, J. Electron Spectrosc. Relat. Phenom. 3, 409 (1974).
[6]J. H. Jacob, Phys. Rev. A 8, 226 (1973).
[7]B. L. Henke, J. Phys. (Paris) 32, C4-115 (1971).
[8]J. A. Crowther, Proc. R. Soc. London Ser. A 84, 226 (1910).
[9]R. O. Lane and D. J. Zaffarano, Phys. Rev. 94, 960 (1954).
[10]M. Davis, Phys. Rev. 94, 243 (1954).
[11]F. Rohrlich and B. C. Carlson, Phys. Rev. 93, 38 (1954).
[12]J. R. Young, J. Appl. Phys. 27, 1 (1956).
[13]J. R. Young, Phys. Rev. 103, 292 (1956).
[14]R. W. Varder, Philos. Mag. 29, 725 (1915).
[15]J. S. Marshall and A. G. Ward, Can. J. Res. 15 (3), 39 (1937).
[16]M. Fink and J. Ingram, At. Data 1, 385 (1970).
[17]M. Fink and J. Ingram, At. Data 4, 129 (1972).
[18]H. A. Bethe, M. E. Rose, and L. P. Smith, Proc. Am. Philos. Soc. 78, 573 (1938).
[19]H. A. Bethe and J. Jacob, Phys. Rev. A 16, 1952 (1977).
[20]A. Adams, R. W. Rendell, W. P. West, H. P. Boida, P. K. Hansma, and H. Metiu, Phys. Rev. B 21, 5565 (1980).
[21]R. C. Longsworth, in Proceedings of the American Vacuum Society, New Jersey, May 1976 (unpublished).
[22]C. B. Opal, E. C. Beaty, and W. K. Peterson, At. Data 4, 209 (1972).
[23]L. Pages, E. Bertel, H. Jaffre, and L. Sklavenitis, At. Data 4, 1 (1972).
[24]R. W. G. Wyckoff, *Crystal Structures*, 2nd ed. (Interscience, New York, 1963).
[25]*American Institute of Physics Handbook*, 2nd ed., edited by D. W. Gray (McGraw-Hill, New York, 1963), pp. 2–21.
[26]M. S. Livingston and H. A. Bethe, Rev. Mod. Phys. 9, 263 (1937).
[27]M. F. Mott, Proc. Cambridge Philos. Soc. 27, 553 (1931).
[28]L. J. Kieffer, *Bibliography of Low Energy Electron and Photon Cross Section Data*, Natl. Bur. Stand Special Publication No. 426, 1976.